

References

- Chen, L. B., and Buchanan, J. M. (1975), *Proc. Natl. Acad. Sci. U.S.A.* 72, 1132.
- Christman, J. K., and Acs, G. (1974), *Biochim. Biophys. Acta* 340, 339.
- Cuatrecasas, P., Wilcheck, M., and Anfinsen, C. B. (1968), *Proc. Natl. Acad. Sci. U.S.A.* 61, 636.
- Davis, B. J. (1964), *Ann. N.Y. Acad. Sci.* 121, 304.
- Deutsch, D., and Mertz, E. T. (1970), *Science* 170, 1095.
- Hummel, B. C. W. (1959), *Can. J. Biochem. Physiol.* 37, 1393.
- Lesuk, A., Termineillo, L., Traver, J. H., and Groff, J. L. (1967), *Thromb. Diath. Haemorrh.* 18, 293.
- Lowry, O. H., Rosebrough, N. J., Farr, A. L., and Randall, R. J. (1951), *J. Biol. Chem.* 193, 265.
- Mochan, B., Maciag, T., Iyengar, M. R., and Pye, E. K. (1975), *Fed. Proc., Fed. Am. Soc. Exp. Biol.* 34, 532, No. 1759.
- Nilsson, U. R., Tomar, R. H., and Taylor, F. B., Jr. (1972), *Immunochemistry* 9, 709.
- Ossowski, L., Unkeless, J. C., Tobia, A., Quigley, J. P., Rifkin, D. B., and Reich, E. (1973), *J. Exp. Med.* 137, 112.
- Quigley, J. P., Ossowski, L., and Reich, E. (1974), *J. Biol. Chem.* 249, 4306.
- Schultz, D. R., Wu, M.-C., and Yunis, A. A. (1975), *Exp. Cell Res.* 96, 47.
- Sherry, S., Alkjaersig, N., and Fletcher, A. P. (1964), *J. Lab. Clin. Med.* 64, 145.
- Siegelman, A. M., Calson, A. S., and Robertson, T. (1962), *Arch. Biochem. Biophys.* 97, 159.
- Summaria, L., Arzadon, L., Bernabe, P., and Robbins, K. C. (1975), *J. Biol. Chem.* 250, 3988.
- Summaria, L., Hsieh, B., and Robbins, K. C. (1967), *J. Biol. Chem.* 242, 4279.
- Unkeless, J. C., Dano, K., Kellerman, G. M., and Reich, E. (1974), *J. Biol. Chem.* 249, 4295.
- Unkeless, J. C., Tobia, A., Ossowski, L., Quigley, J. P., Rifkin, D. B., and Reich, E. (1973), *J. Exp. Med.* 137, 85.
- Waddell, W. J. (1956), *J. Lab. Clin. Med.* 48, 311.
- Walther, P. J., Steinman, H. M., Hill, R. L., and McKee, P. A. (1974), *J. Biol. Chem.* 249, 1173.
- Weber, K., and Osborn, M. (1969), *J. Biol. Chem.* 244, 4406.
- Wrigley, C. W. (1971), *Methods Enzymol.* 22, 559.
- Wu, M.-C., Schultz, D. R., Arimura, G. K., Gross, M. A., and Yunis, A. A. (1975), *Exp. Cell Res.* 96, 37.
- Wu, M.-C., Schultz, D. R., and Yunis, A. A. (1976), in *Cancer Enzymology*, Vol. 12, Miami Winter Symposia, Schultz, J., and Ahmad, F., Ed., New York, N.Y., Academic Press, p 25.
- Yunis, A. A., Arimura, G. K., and Russin, D. J. (1977), *Int. J. Cancer* 19, 128.
- Yunis, A. A., Schultz, D. R., and Sato, G. H. (1973), *Biochem. Biophys. Res. Commun.* 52, 1003.

Analysis and Computer Simulation of Aerobic Oxidation of Reduced Nicotinamide Adenine Dinucleotide Catalyzed by Horseradish Peroxidase[†]

Ken-nosuke Yokota^{*†} and Isao Yamazaki

ABSTRACT: Under suitable experimental conditions the aerobic oxidation of NADH catalyzed by horseradish peroxidase occurred in four characteristic phases: initial burst, induction phase, steady state, and termination. A trace amount of H₂O₂ present in the NADH solution brought about initial burst in the formation of oxypoxidase. About 2 mol of oxypoxidase was formed per mol of H₂O₂. When a considerable amount of the ferric enzyme still remained, the initial burst was followed by an induction phase. In this phase the rate of oxypoxidase formation from the ferric enzyme increased with the decrease of the ferric enzyme and an approximately exponential increase of oxypoxidase was observed. A rapid oxidation of NADH suddenly began at the end of the induction phase and the oxidation continued at a relatively constant rate. In the steady

state, oxygen was consumed and H₂O₂ accumulated. A drastic terminating reaction suddenly set in when the oxygen concentration decreased under a certain level. During the reaction, H₂O₂ disappeared accompanying an accelerated oxidation of NADH and the enzyme returned to the ferric form after a transient increase of peroxidase compound II. Time courses of NADH oxidation, O₂ consumption, H₂O₂ accumulation, and formation of enzyme intermediates could be simulated with an electronic computer using 11 elementary reactions and 9 rate equations. The results were also discussed in relation to the mechanism for oscillatory responses of the reaction that appeared in an open system with a continuous supply of oxygen.

The aerobic oxidation of NADH or NADPH catalyzed by plant peroxidases has been investigated mostly in reaction systems containing activators such as Mn²⁺ and certain phe-

nols (Akazawa and Conn, 1958; Williams-Ashman et al., 1959; Klebanoff, 1960; Kalyanaraman et al., 1975). The reaction between horseradish peroxidase and NADH without activators has been studied by Yokota and Yamazaki (1965a). The nature of the reaction is found to be very peculiar. In the presence of a large amount of peroxidase, the oxidation of NADH sets in after a distinct lag period and the reaction comes to a rapid termination on account of O₂ consumption. During the ter-

[†]From the Biophysics Division, Research Institute of Applied Electricity, Hokkaido University, Sapporo 060, Japan. Received November 29, 1976.

[†]Present address: Muroran Institute of Technology, Mizumotocho, Muroran 050, Japan.

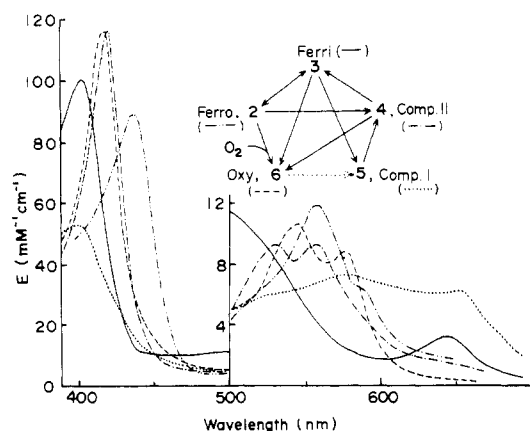


FIGURE 1: Absorption spectra of five oxidation-reduction forms of horseradish peroxidase. Ferriperoxidase, native enzyme; ferropoxidase, the enzyme is reduced by sodium dithionite; compound I, a slight molar excess of H_2O_2 is added to ferropoxidase; compound II, a steady-state form of the enzyme in the presence of H_2O_2 and ascorbic acid; oxypoxidase, 0.5 mM NADH is added to an aerobic solution of ferriperoxidase. (Insert) Five oxidation-reduction states of horseradish peroxidase expressed as a pentagonal diagram (Yamazaki et al., 1973). The numbers on the corners denote the relative oxidation number of the peroxidase heme. $2 + \text{O}_2 \rightarrow 6$, $2 + \text{H}_2\text{O}_2 \rightarrow 4$, $3 + \text{HO}_2 \rightarrow 6$, $3 + \text{H}_2\text{O}_2 \rightarrow 5$, and $4 + \text{H}_2\text{O}_2 \rightarrow 6$; others are one-electron steps. Reaction paths, $3 \rightarrow 5 \rightarrow 4 \rightarrow 3$, indicate a catalytic cycle of the enzyme. Reaction $6 \rightarrow 5$ has not yet been confirmed experimentally.

minating reaction most of the enzyme returns to the original state. This reaction pattern is reminiscent of the mechanism of a pipet washer and it is easy to obtain a reaction system that exhibits damped oscillations (Yamazaki et al., 1965).

Each cycle of the damped oscillations is found to be similar to the reaction that occurs in a closed system containing a small amount of oxygen. The addition of methylene blue and a dehydrogenase system stabilizes the oscillations (Nakamura et al., 1969; Yamazaki and Yokota, 1973) but the analysis of the reaction becomes more difficult. Consequently, to clarify the basic mechanism for the oscillatory responses, this paper deals with a complete analysis of the reaction in a closed system and also in the absence of such stabilizing factors. Characteristic features of the reaction are analyzed kinetically and the overall reaction is simulated with an electronic computer.

For convenience of understanding the present paper, absorption spectra of horseradish peroxidase in five redox states and relations between these states are illustrated in Figure 1.

Materials and Methods

Peroxidase (donor: H_2O_2 oxidoreductase, EC 1.11.1.7) was isolated from wild horseradish roots according to the method of Shannon et al. (1966). The enzyme was purified by CM^1 -cellulose column chromatography and crystallized from an ammonium sulfate solution. The enzyme preparation used in this experiment was a mixture of isoenzymes B and C according to nomenclature by Paul (1958) and Shannon et al. (1966). The ratio of the absorbance at 403 nm to that at 280 nm of the preparation was 3.0.

Superoxide dismutase was kindly supplied by Dr. Sawada in this laboratory. The enzyme was prepared from dry seeds of green pea (*Pisum sativum*) and the concentration of the enzyme was calculated from $E_{680\text{nm}} = 0.29 \text{ mM}^{-1} \text{ cm}^{-1}$ (Sawada et al., 1972).

In most cases absorbance changes at two wavelengths were

¹ Abbreviation used: CM, carboxymethyl.

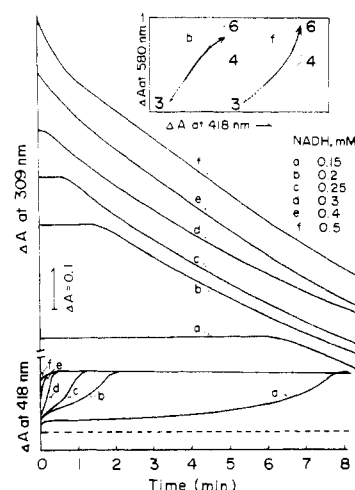


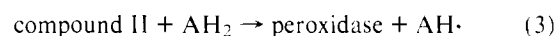
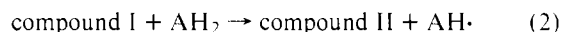
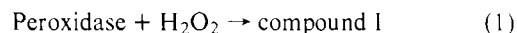
FIGURE 2: The effect of the initial NADH concentration on the reaction pattern of peroxidase-catalyzed aerobic oxidation of NADH. NADH was added to an aerobic solution containing $2.8 \mu\text{M}$ peroxidase. The NADH oxidation was measured spectrophotometrically at 309 nm. At this wavelength absorbance of NADH was about one-half of that at 340 nm and was practically unaffected from the states of peroxidase. The NADH concentration is indicated in the figure and the starting point of absorbance at 309 nm is arbitrary. The formation of enzyme intermediates was measured at 418 nm. The broken line indicates the level of the ferric enzyme. The insertion (top): the enzyme intermediates were also assayed by following absorbance simultaneously at 418 and 589 nm. These are recorded with an X-Y recorder in triangle diagrams. The abscissa and ordinate are absorbance at 418 and 580 nm, respectively. The ordinate scale was expanded by 10. The details are described in the text.

measured simultaneously by the use of a Hitachi two-wavelength spectrophotometer, Model 356. For stopped-flow experiments, a Union Giken rapid reaction analyzer, RA 1300, was used. The apparatus was slightly modified in order to monitor the absorbance of the reaction solutions before mixing.

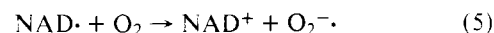
All experiments were carried out at 25°C in 0.1 M sodium acetate, pH 5.6.

Results

When hydrogen peroxide is added to a peroxidase solution in the presence of a hydrogen donor (AH_2), the following catalytic cycle is observed in most cases (George, 1952; Chance, 1952; Yamazaki et al., 1960).



As reaction 2 is much faster than reaction 3, the enzyme intermediate which appears in the steady state is compound II. This is also the case where the hydrogen donor is NADH. Under aerobic conditions, however, the one-electron oxidized form of NADH ($\text{NAD}\cdot$) reacts with O_2 (Yokota and Yamazaki, 1965a; Land and Swallow, 1971) to form a superoxide anion radical.



Reaction 5 has been considered to be essential to the consumption of O_2 in the peroxidase-catalyzed aerobic oxidation of NADH.

In the absence of added H_2O_2 , the peroxidase-oxidase reaction, in most cases, occurred after an induction period. Figure 2 shows time courses of NADH oxidation and oxypoxidase

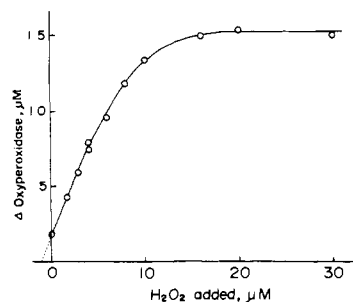


FIGURE 3: Stoichiometric relation between H_2O_2 added and oxypoxidase formed in the initial burst. A mixed solution of NADH (0.4 mM) and H_2O_2 (the concentration is indicated in the abscissa) was added to an aerobic solution containing 17 μM peroxidase. The amount of oxypoxidase accumulated during the initial burst was measured from an absorbance increase at 452 nm (an isosbestic point of the ferric enzyme, compounds I and II).

formation in the presence of varied amounts of NADH. Though oxypoxidase and compound II have similar absorption spectra in the Soret region (Figure 1), the increase of absorbance at 418 nm during the induction period has been confirmed to be due mostly to the formation of oxypoxidase by scanning the spectrum over the visible range (Yokota and Yamazaki, 1965a). The inserted traces in Figure 2 demonstrate changes in the enzyme composition during the increasing phase of absorbance at 418 nm. The abscissa and ordinate denote differences in absorbance at 418 and 580 nm from that of the ferric enzyme, respectively. Consequently, each corner of the triangles represents coordinate of the ferric enzyme for 3, compound II for 4, or oxypoxidase for 6. The experiments were performed using a two-wavelength spectrophotometer as a mode of double monochrometers. Solid lines with an arrow are traces of absorbance changes at 418 and 580 nm recorded in an X-Y recorder. The inserted traces (b and f) show that a considerable amount of compound II accumulated during the formation of oxypoxidase and the amount varied with the concentration of NADH. The ferrous enzyme and compound I were not detectable under these experimental conditions.

Figure 2 shows that the induction phase disappeared when the initial concentration of NADH was higher than 0.4 mM. It is also shown that the time when the oxidation set in was closely related to a rapidly increasing phase of absorbance at 418 nm. The initial burst in the 418-nm absorbance increase appeared to be caused by H_2O_2 accumulated during aging of NADH solutions, because the initial burst was removed by preincubation of the NADH solution with catalase and was augmented by a supplemental addition of H_2O_2 . H_2O_2 was found to be formed from autooxidation of NADH and, on the other hand, consumed for oxidizing NADH. Consequently, the amount of H_2O_2 in an NADH solution reached a constant level about 1 h after preparing the NADH solution. The amount depended on aging conditions of the stock solution.

The addition of a small amount of H_2O_2 with excess NADH to an aerobic solution of peroxidase resulted in a transient appearance of compound II, followed by an accumulation of oxypoxidase. The stoichiometric relation between amounts of H_2O_2 and of oxypoxidase formed during the initial burst was investigated at a high concentration of peroxidase. The result is shown in Figure 3. By extrapolation of the curve, the amount of H_2O_2 per 0.4 mM NADH was estimated at 1.4 μM . The slope in Figure 3 also demonstrates that the mole ratio $\Delta[\text{oxypoxidase}]/\Delta[\text{H}_2\text{O}_2]$ was about 1.6.

Characteristic features of the subsequent slow formation

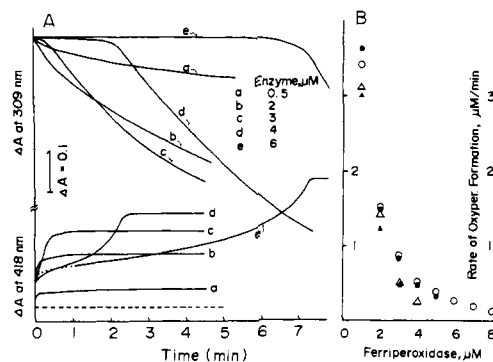
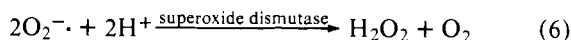


FIGURE 4: (A) The effect of the peroxidase concentration on the reaction pattern of peroxidase-catalyzed aerobic oxidation of NADH. NADH (0.25 mM) was added to aerobic solutions containing varying amounts of peroxidase (indicated in the figure). The NADH oxidation was measured spectrophotometrically at 309 nm and the formation of enzyme intermediates at 418 nm. The broken line indicates the level of the ferric enzyme. (B) The effect of the concentration of remaining ferriperoxidase on the rate of the formation of oxypoxidase. Data are replotted from results analogous to A. The initial concentrations of the enzyme were 5 (\blacktriangle), 6 (\triangle), 7 (\bullet), and 10 (\circ) μM .

of oxypoxidase are demonstrated in Figure 4. Figure 4A shows time courses of NADH oxidation and oxypoxidase formation in the presence of varied amounts of the enzyme. The induction period disappeared at enzyme concentrations below 2 μM and the rate of NADH oxidation in the steady state was proportional to the enzyme concentration up to 6 μM . The formation of oxypoxidase apparently obeyed kinetics of autocatalytic reactions. Of special interest was the factor that controlled the rate of the formation. In Figure 4B the rate of oxypoxidase formation during the induction phase is plotted against the concentration of ferriperoxidase remaining in the reaction solution; the total concentration of the enzyme varied from 5 to 10 μM . It may be concluded that the rate of oxypoxidase formation greatly depended on the ferriperoxidase concentration but only slightly on the concentration of oxypoxidase present in the solution at that time. The rate of 0.1 $\mu\text{M min}^{-1}$ was measured in the presence of 8 μM ferriperoxidase; the value was approximately equal to the rate of NADH autooxidation measured in the absence of peroxidase.

It has been reported (Odajima, 1971; Yamazaki and Yamazaki, 1973) that the NADH oxidation is inhibited by superoxide dismutase accelerating disproportionation of $\text{O}_2^{\cdot-}$ (McCord and Fridovich, 1969). Figure 5 demonstrates the effect of superoxide dismutase on the oxidation of NADH caused by varied amounts of H_2O_2 . By the presence of superoxide dismutase, the initial rate of the NADH oxidation was not much affected but the oxidation of NADH became inhibited with time (compare solid and broken curves c in Figure 5). In the presence of 1.2 μM superoxide dismutase only a part of peroxidase was converted to oxypoxidase during the initial burst in the NADH oxidation and after that the oxidation was strongly inhibited (Figure 5, c-e). The amount of NADH oxidized during the initial burst in the presence of superoxide dismutase was nearly proportional to the amount of H_2O_2 added (insert in Figure 5); the mole ratio $\Delta[\text{NADH}]/\Delta[\text{H}_2\text{O}_2]$ was about 7. If the NADH oxidation was composed of reactions 1, 2, 3, 5, and 6



the reaction should continue of its own accord. The finite value

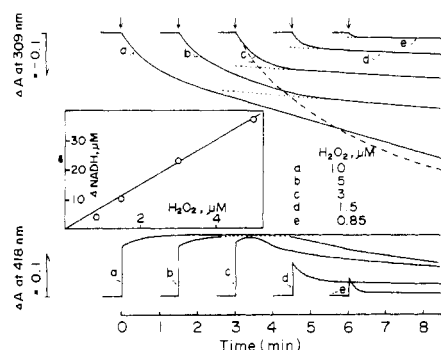
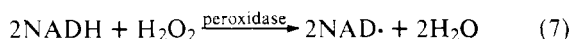


FIGURE 5: The effect of the H_2O_2 concentration on the reaction pattern of peroxidase-catalyzed aerobic oxidation of NADH in the presence of superoxide dismutase. The reaction was started by an addition of H_2O_2 (the concentration is indicated in the figure) to an aerobic solution containing 0.3 mM NADH, 2.5 μM peroxidase, and 1.2 μM superoxide dismutase. The NADH oxidation was measured spectrophotometrically at 309 nm and the formation of enzyme intermediates at 418 nm. The time when the reaction was started is indicated by an arrow. The oxidation of NADH in the absence of superoxide dismutase is shown in the case of c as a broken line. The insertion: the stoichiometric relation between H_2O_2 added and NADH oxidized during the rapid reaction. The ordinate value was obtained by extrapolating the 309-nm trace in the slow reaction phase at the starting point, as demonstrated by dotted lines in the upper traces.

of the ratio implies an involvement of chain termination.

Although oxypoxidase is not an active intermediate, its decomposition occurs when the concentration of O_2 decreases nearly to zero (Yokota and Yamazaki, 1965a). Figure 6 shows a characteristic reaction pattern which appeared when the reaction was started in the presence of suitable amounts of peroxidase, NADH and O_2 . In this figure are shown appearance and disappearance of various molecules, such as NADH, O_2 , H_2O_2 , compound II, and oxypoxidase. This reaction apparently consisted of four phases: initial burst, induction phase, steady state, and termination. The wavelengths of 452 and 463 nm are isosbestic between ferriperoxidase and compound II and between ferriperoxidase and oxypoxidase, respectively. The decrease in absorbance at 463 nm thus denotes the formation of compound II (see Figure 1). It should be noted that compound II was not detectable in the induction phase. Oxypoxidase reached a maximum level slightly after the end of the induction phase and then gradually decreased in the steady state. A shoulder of the 452-nm trace in the terminating reaction may be ascribed to a temporary appearance of a small amount of ferriperoxidase. After the terminating reaction most of the enzyme returned to the ferric state but about 20% of the enzyme was left in the form of oxypoxidase, which gradually decomposed to the ferric enzyme.

From the trace of absorbance at 309 nm (Figure 6), the rate of NADH oxidation in the steady state was measured to be 1.2 $\mu\text{M s}^{-1}$. It would be of interest to compare the value with that of the rate of NAD^\bullet radical formation. As described already, the reaction of NADH with compound II is rate limiting in the overall reaction composed of reactions 1, 2, and 3. The overall reaction can be expressed as



Kinetic experiments revealed that the rate of reaction 3 obeyed approximately the following equation when the electron donor was NADH

$$-\frac{d[\text{compound II}]}{dt} = k_3[\text{NADH}][\text{compound II}] \quad (8)$$

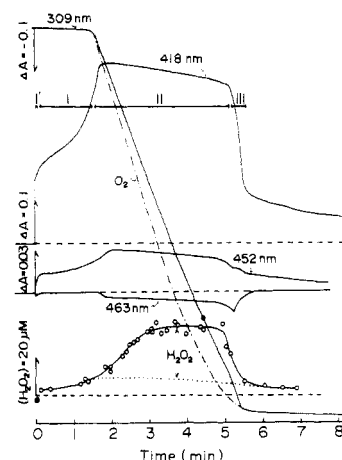


FIGURE 6: Analysis of one-cycle of oscillatory responses in the peroxidase system. The reaction was started by an addition of 0.43 mM NADH to a solution containing 6.8 μM peroxidase and 0.15 mM O_2 . The NADH oxidation was measured spectrophotometrically at 309 nm and the O_2 concentration was calculated using the relation, $-2\Delta[\text{O}_2] = -\Delta[\text{NADH}] + \Delta[\text{H}_2\text{O}_2]$. H_2O_2 was assayed with a guaiacol method using a stopped-flow apparatus. An aliquot of the reaction mixture at a given reaction time was mixed with a 10 mM guaiacol solution and the increase of absorbance at 463 nm was recorded. The absorbance reached a maximum level within a second and then gradually decreases. The amount of H_2O_2 given in the ordinate of the bottom figure was estimated from the maximum absorbance using the standard titration curve with H_2O_2 . Since the colored product is also formed from the reactions of guaiacol with compound II and oxypoxidase, the real concentration of H_2O_2 present in the reaction mixture is given as an interval between the solid and dotted lines. The dotted line is calculated as the sum of $\frac{1}{2}[\text{compound II}]$ and $\frac{1}{2}[\text{oxypoxidase}]$ (Yamazaki et al., 1968). Compound II and oxypoxidase were followed spectrophotometrically at 463 and 452 nm, respectively. The absorbance change at 418 nm is approximately equal to the sum of those of compound II and oxypoxidase. The reaction can be separated into four phases: I, initial burst; II, induction phase; III, steady state; IV, termination.

where k_3 was determined to be $8 \times 10^2 \text{ M}^{-1} \text{ s}^{-1}$ at pH 5.6. As $[\text{NADH}] = 0.4 \text{ mM}$ and $[\text{compound II}] = 1 \mu\text{M}$ at the beginning of the steady state (Figure 6), the rate of the radical formation through reaction 7 was calculated to be $0.64 \mu\text{M s}^{-1}$.

It should be noticed that the terminating reaction brought about characteristic changes, such as complete disappearance of compound II through its transient increase, accelerated decomposition of oxypoxidase, complete decomposition of H_2O_2 , and accelerated oxidation of NADH. The amount of remaining oxypoxidase at the end of the terminating reaction depended on the experimental conditions. Figure 7 shows the effect of the NADH concentration on the terminating reaction. Though each NADH concentration in the experiment of Figure 7 appeared to be enough to bring complete anaerobiosis, the reaction pattern was sensitive to a small change in the NADH concentration. The complete recovery of the ferric enzyme was observed when the initial concentration of NADH was above 0.7 mM but 0.65 mM NADH was not enough for that. At a fixed concentration of NADH, the recovery of the ferric enzyme became incomplete when the enzyme concentration was high. When the initial concentration of NADH was 0.8 mM, the complete recovery of the ferric enzyme was observed in the case of 7 μM peroxidase (Figure 7) but not in the case of 9.8 μM peroxidase.

Discussion

Problems in Analyzing the Mechanism of Oscillatory Oxidation of NADH. From kinetic results of absorbance at 418

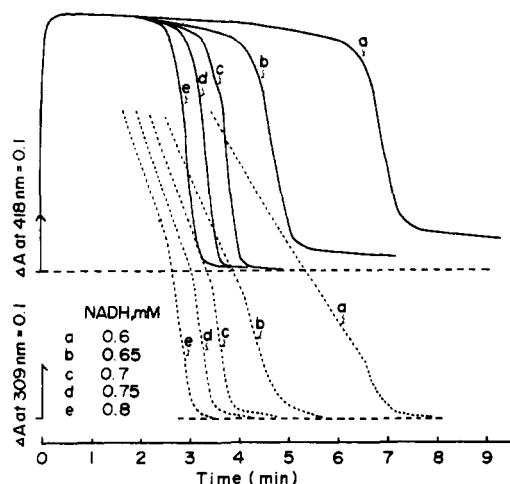


FIGURE 7: The effect of the NADH concentration on the terminating (recovering) reaction. Varying amounts of NADH were added to an aerobic solution containing $7 \mu\text{M}$ peroxidase. The formation of enzyme intermediates was measured spectrophotometrically at 418 nm and the NADH oxidation at 309 nm. The upper broken line indicates the level of the ferric enzyme. For ready comparison the final levels of absorbance at 309 nm are displayed by the same line (the lower broken line).

nm, it was suggested that oxypoxidase plays an essential role in the oscillatory oxidation of NADH (Yamazaki and Yokota, 1967). This view, however, has been criticized by Degn (1969) and Degn and Mayer (1969). Degn (1969) has reported that damped oscillations occur in the aerobic oxidation of not only NADH, but also dihydroxyfumaric acid or indole-3-acetic acid in spite of the fact that time courses of the oxypoxidase concentration during the reactions are considerably different.

In these experiments (Yamazaki and Yokota, 1967; Degn, 1969), the enzyme intermediate was monitored at 418 nm and the results were analyzed on the basis of an assumption that the increase of 418-nm absorbance is due to the formation of oxypoxidase. This assumption is true under specified conditions (Yokota and Yamazaki, 1965a), but it has not been confirmed during the all reaction time. Since the Soret absorption bands of oxypoxidase and peroxidase compound II are similar, the distinction between the two enzyme intermediates is necessitated in order to elucidate the mechanism of oscillatory reactions.

From a marked characteristic of the reaction shown in Figure 6, it would be evident that mechanisms which cause induction and termination are closely related to the oscillatory sources in the aerobic oxidation of NADH catalyzed by peroxidase. The initial burst is not involved in the oscillatory reaction but the key to the mechanism of oxypoxidase formation will be afforded by analysis of the reaction.

Initial Burst. The primary oxidation product of NADH in reaction 7 is a free radical species that acts as a strong reductant or disproportionates in the absence of an appropriate electron acceptor. The second-order rate constant for the reaction of the NAD^\bullet radical with O_2 (k_5) has been measured as $2.0 \times 10^9 \text{ M}^{-1} \text{ s}^{-1}$ by pulse radiolysis at pH 8.4 (Land and Swallow, 1971). The formation of oxypoxidase from the reaction between ferriperoxidase and O_2^\bullet has been suggested in a peroxidase-dihydroxyfumarate system (Yamazaki and Piette, 1963), and its rate constant (k_9) has been measured roughly as $3.2 \times 10^7 \text{ M}^{-1} \text{ s}^{-1}$ at pH 5.5 from the steady-state kinetics at varied concentrations of superoxide dismutase (Sawada and Yamazaki, 1973).

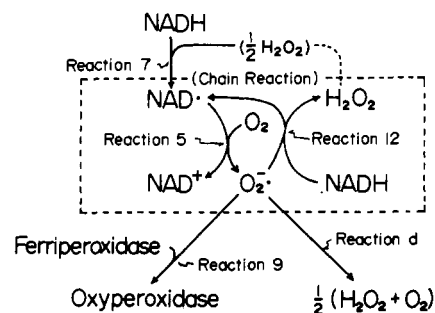
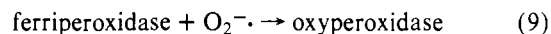
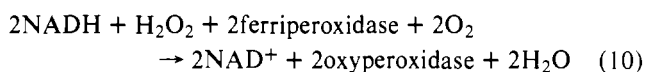


FIGURE 8: Reactions related to the transition from the induction phase to the steady state. Proton balance is not shown in this scheme. Refer to eq 13 in the text.



If the overall reaction in the initial burst is composed of reactions 7, 5, and 9, the stoichiometry of the reaction is



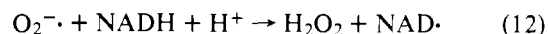
The mole ratio $\Delta[\text{oxypoxidase}]/\Delta[\text{H}_2\text{O}_2]$ estimated from Figure 3 is 1.6, the value being slightly less than the theoretical value. Similar observation has been reported in a peroxidase-dihydroxyfumarate system (Yamazaki and Piette, 1963). The ratio appears to approach the theoretical value in a reaction system where H_2O_2 is supplied slowly and homogeneously.

Induction Phase. It seems that the induction period depends on the mole ratio of peroxidase to H_2O_2 present in the NADH solution. The induction phase disappears when the ratio is less than about 0.5 (see Figures 2 and 4). Characteristic features of the induction phase are: (1) the rate of oxypoxidase formation depends mostly on the concentration of the ferric enzyme (Figure 4B), and (2) neither H_2O_2 nor compound II is detectable (Figure 6). The oxidizing capacity of the reaction solution in this phase (see Figure 6) is ascribed to oxypoxidase. Oxypoxidase can act as a trivalent oxidant for guaiacol (Yokota and Yamazaki, 1965b; Yamazaki et al., 1968).

During the induction phase, the oxidation of NADH is very slow and the curve of oxypoxidase formation is analogous to that of bacterial growth. If the autoxidation of NADH is formulated as



the rate of oxypoxidase formation will be nearly twice that of NADH autoxidation in the presence of a sufficient amount of ferriperoxidase. The abnormal dependence of the rate of the oxypoxidase formation on the concentration of ferriperoxidase (Figure 4B) would be accounted for by assuming competition of reactions 9 and 12.



Reaction 12 appears to be an essential reaction in propagation of the chain reaction, which results in the overall increase of oxypoxidase. According to the mechanism demonstrated in Figure 8 and assuming that the NAD^\bullet radical disappears only through reaction 5, the gain of the O_2^\bullet production can be formulated by

gain

$$= \frac{3k_{12}[\text{NADH}][\text{O}_2^\bullet] + k_d[\text{O}_2^\bullet]^2}{k_{12}[\text{NADH}][\text{O}_2^\bullet] + k_9[\text{ferriperoxidase}] \times [\text{O}_2^\bullet] + k_d[\text{O}_2^\bullet]^2} \quad (13)$$

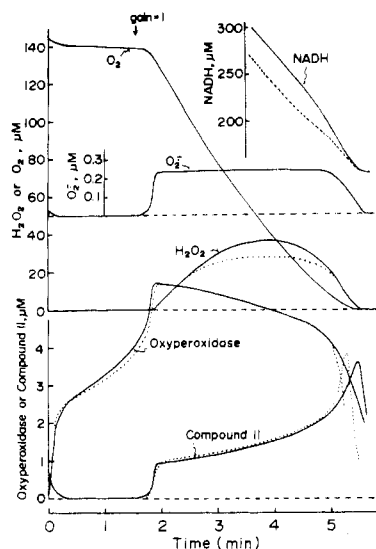
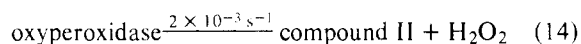


FIGURE 9: Computer simulation of reaction curves shown in Figure 6. The values of parameters used for this calculation are shown in the Appendix. Solid lines are calculated and dotted lines show experimental data. The time at which the gain in eq 13 becomes unity is indicated by an arrow. The time course of NADH oxidation is shown only in the terminating part of the reaction.

In the induction phase every reaction occurs so slowly that the square term of $[O_2^{\cdot-}]$ appears to be negligible in the absence of superoxide dismutase. Assuming that the gain approaches unity when the concentration of remaining ferriperoxidase is 10^{-6} M (Figure 4B), the ratio k_9/k_{12} is estimated to be about 600. If $k_9 = 3.2 \times 10^7 \text{ M}^{-1} \text{ s}^{-1}$, k_{12} is calculated to be $6 \times 10^4 \text{ M}^{-1} \text{ s}^{-1}$. However, Land and Swallow (1971) have reported that $k_{12} < 27 \text{ M}^{-1} \text{ s}^{-1}$ at pH 8.4. This seems a serious discrepancy but it might be explained by two reasons. (1) The value of $3.2 \times 10^{-7} \text{ M}^{-1} \text{ s}^{-1}$ for k_9 is overestimated (Sawada and Yamazaki, 1973). (2) Reaction 12 appears to depend greatly on pH and becomes much faster as the pH decreases. Bielski and Chan (1973, 1974) have reported that a chain oxidation of NADH by $O_2^{\cdot-}$ through reactions 5 and 12 occurs in the presence of lactate dehydrogenase.

The above mechanism for the formation of oxyperoxidase is still insufficient to explain the whole feature of the induction phase. The data of Figure 4B, particularly those in the presence of 3 and 4 μM ferriperoxidase, indicate that the rate of oxyperoxidase formation slightly depends on the concentration of oxyperoxidase. It has been reported by Tamura and Yamazaki (1972) that the autodecomposition of oxyperoxidase is initiated by reaction 14.



This reaction is slow but must be reckoned with after the concentration of oxyperoxidase reaches a certain level. Since the products of reaction 14 yield three molecules of the NAD \cdot radical through reactions 3 and 7, reaction 14 results in an overall increase of 2 mol of oxyperoxidase.

When the concentration of ferriperoxidase lowers to about 1 μM , H_2O_2 begins to accumulate, compound II appears, and the reaction is transferred to the steady state.

Steady State. In the steady state, the reaction of $O_2^{\cdot-}$ with ferriperoxidase becomes negligible. The overall increase of H_2O_2 , however, cannot be expected unless a chain reaction that consists of reactions 5 and 12 does take place. Since reaction 5 is very fast, the maintenance of the chain reaction is practi-

cally affected by the rate of reaction 12. Reaction 12 becomes negligible in the presence of superoxide dismutase.

It seems that the oxidation of NADH occurs through both reactions 7 and 12. The rate of the oxidation through reaction 7 can be formulated as

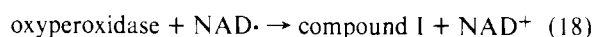
$$v = 2k_3(\text{NADH})(\text{compound II}) \quad (15)$$

since $v = 0.56 \mu\text{M s}^{-1}$ and the maximum rate of H_2O_2 accumulation is $0.3 \mu\text{M s}^{-1}$ (Figure 6), the rate of NADH oxidation, calculated as the sum of reactions 7 and 12, will be less than $0.86 \mu\text{M s}^{-1}$. This value is lower than that estimated directly from Figure 6. This difference may be accounted for by introducing the following reactions.

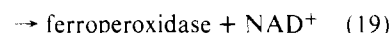
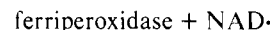


These reactions are actually introduced through a process of computer simulation in order to explain the relative constancy of the H_2O_2 concentration in the steady state. Calculation of rate constant for reaction 16 is described in the Appendix. Since reaction 17 is expected to be very fast, it is assumed that reaction 16 causes overall consumption of 1 mol of NADH but no change in balance of the NAD \cdot radical.

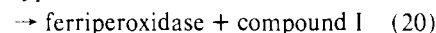
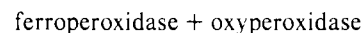
Terminating (or Recovering) Reaction. It seems that rapid changes in this phase are caused by the reducing capacity of the NAD \cdot radical, the steady-state concentration of which increases as the reaction solution approaches anaerobiosis. Though direct conversion from oxyperoxidase to compound I has not yet been confirmed, it is likely that oxyperoxidase is reduced by the NAD \cdot radical. The reaction can tentatively be formulated as



The decrease of H_2O_2 , the decomposition of oxyperoxidase, and the accelerated oxidation of NADH are observed during the whole period of the terminating reaction. However, traces of absorbance at 452 and 463 nm in Figure 6 clearly show that the reaction is composed of two phases. Compound II increases in the former half and decreases in the latter half. Sharp discontinuity in the middle point can be ascribed to a temporary formation of a small amount of reduced peroxidase by the NAD \cdot radical.



Ferriperoxidase reacts with oxyperoxidase at a considerable speed (Yamazaki et al., 1966; Wittenberg et al., 1967). This reaction is tentatively formulated as



Computer Simulation. From the above analysis of the reaction in each step, it may be concluded that each characteristic pattern is accounted for by a combination of several elementary reactions. The overall reaction is thus composed of quite a number of elementary reactions and it is very likely that each reaction takes place not only in one phase but also in all other phases, even though the extent of its contribution may be different in each phase. From this point of view, it becomes very important to confirm whether or not the various features of the overall reaction can be simulated from all of these elementary reactions. The result of computer simulation is shown in Figure 9. The process of the simulation is described in the Appendix.

Simulated time courses of various chemical species are found to coincide with the experimental data, except for small deviation in the H_2O_2 concentration and delay of the terminating phase. The discrepancy is not solved yet, but it would not appear so serious. It is of interest to note that computer simulation tells us accumulation of about $0.23 \mu\text{M}$ $\text{O}_2^{\cdot-}$ in the steady state of the reaction shown in Figure 6. The involvement of $\text{O}_2^{\cdot-}$ has been suggested in physiological reactions containing myeloperoxidase (Odajima, 1971; Klebanoff, 1974; Rotilio et al., 1975) or polymorphonuclear leucocyte (Allen et al., 1974; Yost and Fridovich, 1974; Patriarca et al., 1975; Takanaka and O'Brien, 1975). The formation of $\text{O}_2^{\cdot-}$ in the peroxidase-dihydroxyfumarate reaction has been confirmed by electron spin resonance spectroscopy (Nilsson et al., 1969).

Degn (1969), observing oscillatory oxidation of indole-3-acetic acid, has concluded that oxyperoxidase is not essential in the mechanism of the oscillation. It should be noted that spectrophotometric analysis of the enzyme intermediates becomes more complex when indole-3-acetic acid is the electron donor because of the formation of an inactive enzyme, called P-670 (Yamazaki and Yamazaki, 1973). Degn and Mayer (1969) have explained the oscillatory responses according to a modified Lotka's model (Lotka, 1910, 1920) having diffusion of the reactant and an autocatalytic reaction. The present results show that autocatalytic types of reactions are involved in both inductive and recovering phases, making the reaction easy to oscillate when oxygen is supplied continuously. In both phases oxyperoxidase plays important roles. Preliminary calculation has shown that damped oscillations are simulated when an equation for a continuous supply of oxygen is added to the program used in calculation of the data in Figure 9. The details will be reported elsewhere.

Acknowledgment

We thank Dr. Yukiharu Sawada for supplying superoxide dismutase. Thanks are also due to the committee of computer operation in this institute for the use of FACOM 230-25 computer.

Appendix

Computer Methodology. The differential equations represented below are solved numerically by Runge-Kutta-Gill method on a FACOM 230-25 computer (cycle time = $1.5 \mu\text{s}$) using Fortran language. Since the equation is a kind of "stiff" (Garfinkel et al., 1970) and requires much computer time, the following techniques are used to speed up calculation: (1) the integration step size is variable and automatically controlled so that the calculation error is kept less than a specified limit (0.01%); (2) when calculated variables in several successive steps show a monotonic change, Newton's extrapolation formula is used in place of the Runge-Kutta-Gill method; (3) rate constants for reactions 5, 16, and 18 are divided by 10^5 . This is, in effect, to multiply the NAD^{\cdot} radical concentration by 10^5 and serves for the reduction of computer time.

Finally, about 30 min is required to simulate 300 s of real time.

Initial conditions are equal to those in Figure 6.

Program. The following rate equations are used.

$$\begin{aligned} d[\text{compound I}]/dt &= k_1[\text{H}_2\text{O}_2][\text{ferriperoxidase}] \\ &+ k_{18}[\text{NAD}^{\cdot}][\text{oxyperoxidase}] - k_2[\text{NADH}][\text{compound I}] \end{aligned}$$

$$\begin{aligned} d[\text{compound II}]/dt &= k_2[\text{NADH}][\text{compound I}] \\ &- k_3[\text{NADH}][\text{compound II}] + k_{14}[\text{oxyperoxidase}] \end{aligned}$$

$$\begin{aligned} d[\text{oxyperoxidase}]/dt &= k_9[\text{O}_2^{\cdot-}][\text{ferriperoxidase}] \\ &- k_{14}[\text{oxyperoxidase}] - k_{18}[\text{NAD}^{\cdot}][\text{oxyperoxidase}] \end{aligned}$$

$$\begin{aligned} d[\text{ferriperoxidase}]/dt &= k_3[\text{NADH}][\text{compound II}] \\ &- k_1[\text{H}_2\text{O}_2][\text{ferriperoxidase}] - k_9[\text{O}_2^{\cdot-}][\text{ferriperoxidase}] \end{aligned}$$

$$d[\text{O}_2]/dt = \frac{1}{2}k_d[\text{O}_2^{\cdot-}]^2 - k_5[\text{NAD}^{\cdot}][\text{O}_2]$$

$$\begin{aligned} d[\text{O}_2^{\cdot-}]/dt &= k_5[\text{NAD}^{\cdot}][\text{O}_2] - k_9[\text{O}_2^{\cdot-}][\text{ferriperoxidase}] \\ &- k_{12}[\text{O}_2^{\cdot-}][\text{NADH}] - k_d[\text{O}_2^{\cdot-}]^2 \end{aligned}$$

$$\begin{aligned} d[\text{H}_2\text{O}_2]/dt &= k_{11}[\text{NADH}] + k_{12}[\text{O}_2^{\cdot-}][\text{NADH}] \\ &+ k_{14}[\text{oxyperoxidase}] + \frac{1}{2}k_d[\text{O}_2^{\cdot-}]^2 \\ &- k_1[\text{H}_2\text{O}_2][\text{ferriperoxidase}] - k_{16}[\text{NAD}^{\cdot}][\text{H}_2\text{O}_2] \end{aligned}$$

$$\begin{aligned} d[\text{NAD}^{\cdot}]/dt &= k_2[\text{NADH}][\text{compound I}] \\ &+ k_3[\text{NADH}][\text{compound II}] + k_{12}[\text{O}_2^{\cdot-}][\text{NADH}] \\ &- k_5[\text{NAD}^{\cdot}][\text{O}_2] - k_{18}[\text{NAD}^{\cdot}][\text{oxyperoxidase}] \end{aligned}$$

$$\begin{aligned} d[\text{NADH}]/dt &= -k_2[\text{NADH}][\text{compound I}] \\ &- k_3[\text{NADH}][\text{compound II}] \\ &- k_{12}[\text{O}_2^{\cdot-}][\text{NADH}] - k_{16}[\text{NAD}^{\cdot}][\text{H}_2\text{O}_2] \end{aligned}$$

Parameters are as follows: $k_1 = 1.8 \times 10^7 \text{ M}^{-1} \text{ s}^{-1}$ [Dolman et al. (1975)]; $k_2 = 5.4 \times 10^3 \text{ M}^{-1} \text{ s}^{-1}$; $k_3 = 8.0 \times 10^2 \text{ M}^{-1} \text{ s}^{-1}$; $k_5 = 2.0 \times 10^9 \text{ M}^{-1} \text{ s}^{-1}$ [Land and Swallow (1971)]; $k_9 = 1.9 \times 10^6 \text{ M}^{-1} \text{ s}^{-1}$; $k_{11} = 3.0 \times 10^{-6} \text{ s}^{-1}$; $k_{12} = 5.9 \times 10^3 \text{ M}^{-1} \text{ s}^{-1}$; $k_{14} = 3.0 \times 10^{-4} \text{ s}^{-1}$; $k_{16} = 8.6 \times 10^8 \text{ M}^{-1} \text{ s}^{-1}$; $k_{18} = 1.3 \times 10^8 \text{ M}^{-1} \text{ s}^{-1}$; $k_d = 1.1 \times 10^7 \text{ M}^{-1} \text{ s}^{-1}$ [Rabani and Nielsen (1969)].

Comments to Parameters. k_2 and k_3 . The rates of reactions 2 and 3 are not strictly proportional to the concentration of NADH; but, at low concentrations of NADH, both reactions can be assumed to be first order to NADH. The values for k_2 and k_3 are obtained by measuring the reactions of NADH with compounds I and II, respectively.

k_9 . This value is less than that obtained by Sawada and Yamazaki (1973). First, k_{12} is calculated on the experimental results (see below) and then k_9 is determined so as to make the computer simulation fit to the result.

k_{11} . It is assumed that the rate of reaction 11 is proportional to the concentration of NADH alone. This reaction is very slow and affects the overall reaction only in the induction phase.

k_{12} and k_{16} . The values are obtained as follows. In the steady state, one obtains the following equations.

$$\begin{aligned} d[\text{NAD}^{\cdot}]/dt &= k_{12}[\text{O}_2^{\cdot-}][\text{NADH}] \\ &+ 2k_3[\text{NADH}][\text{compound II}] - k_5[\text{NAD}^{\cdot}][\text{O}_2] = 0 \end{aligned}$$

$$\begin{aligned} d[\text{H}_2\text{O}_2]/dt &= k_{12}[\text{O}_2^{\cdot-}][\text{NADH}] + \frac{1}{2}k_d[\text{O}_2^{\cdot-}]^2 \\ &- k_3[\text{NADH}][\text{compound II}] - k_{16}[\text{NAD}^{\cdot}][\text{H}_2\text{O}_2] = 0 \end{aligned}$$

$$d[\text{O}_2]/dt = \frac{1}{2}k_d[\text{O}_2^{\cdot-}]^2 - k_5[\text{NAD}^{\cdot}][\text{O}_2]$$

$$\begin{aligned} d[\text{NADH}]/dt &= -k_{12}[\text{O}_2^{\cdot-}][\text{NADH}] \\ &- 2k_3[\text{NADH}][\text{compound II}] - k_{16}[\text{NAD}^{\cdot}][\text{H}_2\text{O}_2] \end{aligned}$$

Using the results at a specified time in Figure 6

$$d[\text{O}_2]/dt = -0.6 \mu\text{M s}^{-1}, d[\text{NADH}]/dt = -1.2 \mu\text{M s}^{-1}$$

$$[\text{NADH}] = 237 \mu\text{M}, [\text{compound II}] = 1.5 \mu\text{M}$$

$$[\text{H}_2\text{O}_2] = 25 \mu\text{M}, [\text{O}_2] = 35 \mu\text{M}$$

the simultaneous equation gives solutions:

$$k_3[\text{NADH}][\text{compound II}] = 0.284 \mu\text{M s}^{-1}$$

$$k_5[\text{O}_2][\text{NAD}^{\cdot}] = 0.884 \mu\text{M s}^{-1}$$

$$k_{12}[\text{O}_2^{\cdot-}][\text{NADH}] = 0.315 \mu\text{M s}^{-1}$$

$$k_{16}[\text{NAD}^{\cdot}][\text{H}_2\text{O}_2] = 0.315 \mu\text{M s}^{-1}$$

$$k_d[\text{O}_2^{\cdot-}]^2 = 0.568 \mu\text{M s}^{-1}$$

Then, the steady-state concentrations of $\text{O}_2^{\cdot-}$ and NAD^{\cdot} are calculated as 2.27×10^{-7} and 1.26×10^{-11} M, respectively. And, the values of 5.86×10^3 and $1.00 \times 10^9 \text{ M}^{-1} \text{ s}^{-1}$ are given to k_{12} and k_{16} , respectively. The value of $1.00 \times 10^9 \text{ M}^{-1} \text{ s}^{-1}$ for k_{16} , however, is found to be slightly large to simulate the overall reaction and the value of $8.6 \times 10^8 \text{ M}^{-1} \text{ s}^{-1}$ is used instead.

k_{14} and k_{18} . These values are determined so as to get the best simulation.

References

- Akazawa, T., and Conn, E. E. (1958), *J. Biol. Chem.* **232**, 403.
- Allen, R. C., Yevich, S. J., Orth, R. W., and Steele, R. H. (1974), *Biochem. Biophys. Res. Commun.* **60**, 909.
- Bielski, B. H. J., and Chan, P. C. (1973), *Arch. Biochem. Biophys.* **159**, 873.
- Bielski, B. H. J., and Chan, P. C. (1974), *J. Biol. Chem.* **250**, 318.
- Chance, B. (1952), *Arch. Biochem. Biophys.* **41**, 416.
- Degn, H. (1969), *Biochim. Biophys. Acta* **180**, 271.
- Degn, H., and Mayer, D. (1969), *Biochim. Biophys. Acta* **180**, 291.
- Dolman, D., Newell, G. A., Thurlow, M. D., and Dunford, H. B. (1975), *Can. J. Biochem.* **53**, 495.
- Garfinkel, D., Garfinkel, L., Pring, M., Green, S. B., and Chance, B. (1970), *Annu. Rev. Biochem.* **39**, 473.
- George, P. (1952), *Nature (London)* **169**, 612.
- Kalyanaraman, V. S., Kumar, S. A., and Mahadevan, S. (1975), *Biochem. J.* **149**, 577.
- Klebanoff, S. J. (1960), *Biochim. Biophys. Acta* **44**, 501.
- Klebanoff, S. J. (1974), *J. Biol. Chem.* **249**, 3724.
- Land, E. J., and Swallow, A. J. (1971), *Biochim. Biophys. Acta* **234**, 34.
- Lotka, A. J. (1910), *J. Phys. Chem.* **14**, 271.
- Lotka, A. J. (1920), *J. Am. Chem. Soc.* **42**, 1595.
- McCord, J. M., and Fridovich, I. (1969), *J. Biol. Chem.* **244**, 6049.
- Nakamura, S., Yokota, K., and Yamazaki, I. (1969), *Nature (London)* **222**, 794.
- Nilsson, R., Pick, F. M., and Bray, R. C. (1969), *Biochim. Biophys. Acta* **192**, 145.
- Odajima, T. (1971), *Biochim. Biophys. Acta* **235**, 52.
- Patriarca, P., Dri, P., Kakinuma, K., Tedesco, F., and Rossi, F. (1975), *Biochim. Biophys. Acta* **385**, 380.
- Paul, K. G. (1958), *Acta Chem. Scand.* **12**, 1312.
- Rabani, J., and Nielsen, S. O. (1969), *J. Chem. Phys.* **73**, 3736.
- Rotilio, G., Falcioni, G., Fioretti, E., and Brunori, M. (1975), *Biochem. J.* **145**, 405.
- Sawada, Y., Ohyama, T., and Yamazaki, I. (1972), *Biochim. Biophys. Acta* **268**, 305.
- Sawada, Y., and Yamazaki, I. (1973), *Biochim. Biophys. Acta* **327**, 257.
- Shannon, L. M., Kay, E., and Lew, J. Y. (1966), *J. Biol. Chem.* **241**, 2166.
- Takanaka, K., and O'Brien, P. J. (1975), *Biochem. Biophys. Res. Commun.* **62**, 966.
- Tamura, M., and Yamazaki, I. (1972), *J. Biochem. (Tokyo)* **71**, 311.
- Williams-Ashman, H. G., Cassman, M., and Klavins, M. (1959), *Nature (London)* **184**, 427.
- Wittenberg, J. B., Noble, R. W., Wittenberg, B. A., Antonini, E., Brunori, M., and Wyman, J. (1967), *J. Biol. Chem.* **242**, 626.
- Yamazaki, H., and Yamazaki, I. (1973), *Arch. Biochem. Biophys.* **154**, 147.
- Yamazaki, I., Mason, H. S., and Piette, L. H. (1960), *J. Biol. Chem.* **235**, 2444.
- Yamazaki, I., Nakajima, R., Miyoshi, K., Makino, R., and Tamura, M. (1973), in *Oxidases and Related Redox Systems*, Second Symposium, King, T. E., Mason, H. S., Morrison, M., Ed., Baltimore, Md., University Park Press, p 407.
- Yamazaki, I., and Piette, L. H. (1963), *Biochim. Biophys. Acta* **77**, 47.
- Yamazaki, I., Yamazaki, H., Tamura, M., Ohnishi, T., Nakamura, S., and Iyanagi, T. (1968), *Adv. Chem. Ser. No.* **77**, 290.
- Yamazaki, I., and Yokota, K. (1967), *Biochim. Biophys. Acta* **132**, 310.
- Yamazaki, I., and Yokota, K. (1973), in *Biological and Biochemical Oscillations*, Chance, B., Pye, E. K., Ghosh, A. K., Hess, B., Ed., New York, N.Y., Academic Press, p 109.
- Yamazaki, I., Yokota, K., and Nakajima, R. (1965), *Biochem. Biophys. Res. Commun.* **21**, 582.
- Yamazaki, I., Yokota, K., and Tamura, M. (1966), in *Hemes and Hemoproteins*, Chance, B., Estabrook, R. E., and Yonetani, T., Ed., New York, N.Y., Academic Press, p 319.
- Yokota, K., and Yamazaki, I. (1965a), *Biochim. Biophys. Acta* **105**, 301.
- Yokota, K., and Yamazaki, I. (1965b), *Biochem. Biophys. Res. Commun.* **18**, 48.
- Yost, F. J., Jr., and Fridovich, I. (1974), *Arch. Biochem. Biophys.* **161**, 395.